Alberts *et al. Vessel Plus* 2023;7:34
**DOI:** 10.20517/2574-1209.2023.37

**Vessel Plus**

**Review**

**Open Access**

# Transesophageal echocardiography during surgery of the thoracic aorta in adults

**Tim Alberts, Susanne Eberl, Henning Hermanns**

Department of Anesthesiology, Amsterdam University Medical Centers, Amsterdam 1105AZ, the Netherlands.

**Correspondence to:** Dr. Tim Alberts, Department of Anesthesiology, Amsterdam UMC, Meibergdreef 9, Amsterdam 1105AZ, the Netherland. E-mail: t.alberts@amsterdamumc.nl

**How to cite this article:** Alberts T, Eberl S, Hermanns H. Transesophageal echocardiography during surgery of the thoracic aorta in adults. *Vessel Plus* 2023;7:34. https://dx.doi.org/10.20517/2574-1209.2023.37

**Received:** 23 May 2023 **First Decision:** 14 Nov 2023 **Revised:** 29 Nov 2023 **Accepted:** 19 Dec 2023 **Published:** 25 Dec 2023

**Academic Editor:** Frank W. Sellke **Copy Editor:** Fangyuan Liu **Production Editor:** Fangyuan Liu

## Abstract

Thoracic aortic surgery poses significant challenges due to the complex anatomy and potential for life-threatening complications. Transesophageal echocardiography (TEE) has emerged as a crucial imaging tool in the management of patients undergoing these operations. TEE offers real-time, high-resolution imaging of the heart and aorta, enabling accurate assessment of aortic pathology, evaluation of cardiac function, and monitoring of intraoperative hemodynamics. Its semi-invasive nature, immediate availability, and ability to provide dynamic information make TEE an indispensable adjunct during these intricate procedures. One of the primary indications for TEE during thoracic aortic surgery is the assessment of aortic pathology, including aneurysms, dissections, and aortic valve diseases. TEE allows precise visualization of the extent, location, and severity of aortic lesions, facilitating decision-making regarding repair strategies, graft sizing, and intraoperative guidance. Furthermore, TEE aids in identifying associated cardiac abnormalities such as valvular or ventricular dysfunction, which may impact surgical planning and outcomes. This review aims to summarize the current evidence supporting the use of TEE during thoracic aortic surgical interventions and highlight its invaluable contributions to perioperative patient care.

**Keywords:** Transesophageal echocardiography, thoracic aorta, aorta surgery, cardiovascular surgery, cardiac anesthesia

## INTRODUCTION

Echocardiography is the diagnostic tool of choice for numerous indications such as assessment of

ventricular and valve function, pericardial effusion, or other cardiac abnormalities. During cardiothoracic surgery, transesophageal echocardiography (TEE) is used to confirm known or new pathology, asses heart function, and to evaluate the effect of inotropic or fluid therapy. The use of TEE during cardiac surgery has been shown to be associated with lower mortality and improved patient outcomes[1-3]. Since the greater part of the thoracic aorta can be well visualized by TEE, it proves to be an invaluable imaging tool in aortic surgical procedures.

Technological developments in echocardiography have resulted in real-time, high-quality imaging and precise measurement tools. With the introduction of special matrix array probes for three-dimensional (3D) echocardiography in the late 2000s, it is possible to visualize structures in simultaneous multiplane modes up to detailed real-time 3D images[4-6].

Although echocardiography operates with harmless ultrasound beams, TEE is categorized as a semi-invasive imaging modality due to the insertion of the probe into the patient's body. Nevertheless, several large studies have shown that TEE is associated with a low incidence of complications (< 1.5%), of which the majority are mild upper gastrointestinal complications such as dysphagia or gastric erosion[7-10]. Thus, international guidelines state that TEE should be routinely used in adults without contraindications during surgery on the thoracic aorta[11-14].

Especially in the non-elective setting, surgery of the thoracic aorta is often high-risk surgery, associated with significant blood loss, morbidity, and mortality. This requires optimal teamwork between the surgical, perfusion, and anesthetic teams. For cardiac anesthesiologists, as well as cardiologists and cardiac surgeons, a thorough understanding of the aspects of TEE is essential to guide the aortic procedure, evaluate surgical repair, and screen for possible complications.

In this narrative review, we discuss the different aspects of the use of TEE during surgery of the aorta. We start with a more technical part: The different parts of the thoracic aorta and how to visualize them. Secondly, we address aortic diseases and their appearance on TEE. Finally, we discuss the use of TEE during endovascular surgery of the thoracic aorta.

## ANATOMY AND DEVELOPMENT OF THE AORTA

The thoracic aorta consists of the aortic root and a tubular part. The aortic root is a complex anatomic structure, which includes the aortic valve annulus, leaflets, leaflets attachments, inter-leaflet triangles, sinuses of Valsalva, and the sinotubular junction[15]. It connects the heart to the systemic circulation and gives rise to the coronary arteries. The coronary arteries originate at the left and right sinuses of Valsalva, situated distal to the aortic valve.

The tubular part of the thoracic aorta consists of three segments. The ascending aorta originates at the sinotubular junction and rises up to the brachiocephalic trunk.

The aortic arch begins at the brachiocephalic trunk and runs up to the left subclavian artery. In its course, it gives rise to three branches. In the most common anatomic variant (approximately 80% of the population), the branches of the aortic arch are the brachiocephalic artery, the left common carotid artery, and the left subclavian artery [Figure 1]. In approximately 14% of the population, the left common carotid artery arises from the brachiocephalic artery. In approximately 3% of the population, the left vertebral artery arises directly from the aorta[16].

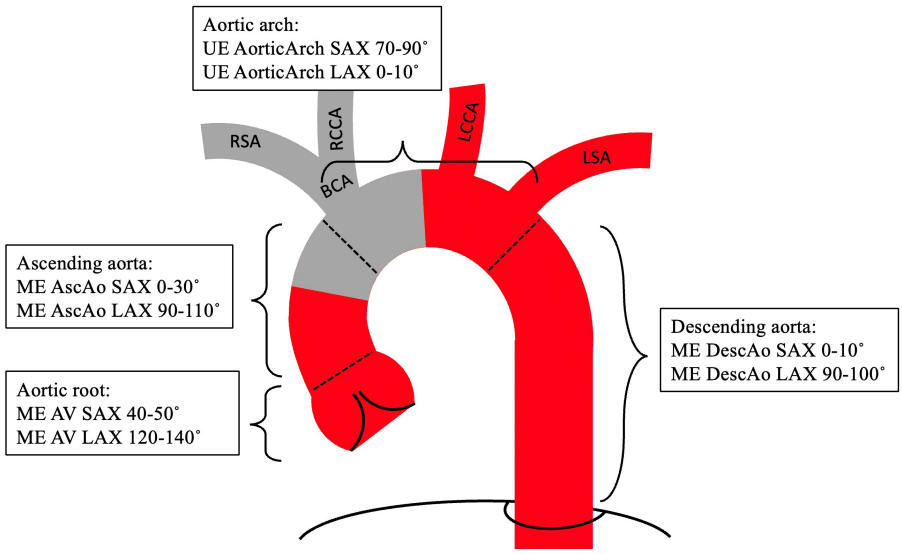


**Figure 1.** Overview of anatomy and the standard views that can be used to visualize the thoracic aorta. AscAo: Ascending aorta; AV: aortic valve; BCA: brachiocephalic artery; LAX: long axis; LCCA: left common carotid artery; LSA: left subclavian artery; ME: mid esophageal; RCCA: right common carotid artery; RSA: right subclavian artery; SAX: short axis, UE: upper esophageal. Grey area: blind spot.

The descending thoracic aorta starts distal to the left subclavian artery and runs down through the diaphragm, where it passes into the abdominal aorta. From the descending aorta arise the posterior intercostal arteries.

### Aortic wall

The aortic wall consists of three layers. The *tunica intima* is the innermost layer, which is directly in contact with the blood flow. It is composed of endothelial cells that form a smooth, non-adhesive surface to help reduce friction as blood flows through the vessel. The *tunica media* is the middle layer, which is composed of smooth muscle cells and elastic fibers. It is responsible for regulating the diameter of the artery and maintaining blood pressure. The *tunica adventitia* is the outermost layer, which is composed of connective tissue and collagen fibers. It provides support and protection to the aorta and attaches it to surrounding structures such as the spine and other blood vessels.

### Aortic dimensions

The diameter of the aorta decreases in its course, being the largest at the aortic root and the narrowest at the abdominal aorta. Aortic dimensions are affected by age, sex, daily workload, body surface area (BSA), and especially body height[17-19]. In ratio to BSA, the upper limit of normal has been defined as 2.1 cm/m$^2$ for the ascending aorta and 1.6-1.8 cm/m$^2$ for the descending aorta[18,20]. In addition, several nomograms, which include age, sex, and BSA, have been published, defining these upper limits more precisely[21-23].

### Aortic embryology

During the embryologic development of the aorta, common cell types and signaling pathways form the common origin of structures of the heart and aorta. Aortic valve and vascular smooth muscle cells show many similarities, and development errors in these primitive cell lines may lead to associated abnormalities[24,25]. For example, an error in the formation of the aortic valve leading to a bicuspid aortic valve is associated with an aneurysm of the proximal thoracic aorta, due to the shared involvement of common cell types in the development of both structures. Conversely, a bicuspid aortic valve is rarely

associated with descending aortic aneurysms, which is formed by different cell types[25].

## ECHOCARDIOGRAPHY OF THE AORTA

When assessing the aorta, it is important to optimize image quality ("knobology"). To improve resolution, image depth should be reduced, focus should be set to the near field and gain should be adjusted so the blood in the lumen is displayed as black on the screen[12]. If possible, increasing the ultrasound frequency (for example, with dynamic frequency tuning) can increase axial resolution, especially in the near field. With optimization of these settings, it is possible to differentiate the layers of the aortic wall; the luminal border of the intima appears as a grey line and the collagen-rich adventitia as a white line[26-28].

### Echocardiography of specific aortic parts

*Aortic root*

The aortic root is best imaged in the mid-esophageal (ME) aortic valve (AV) short axis (SAX) (30-40°) and long axis (LAX) view (120-140°)[12]. In the SAX, the three sinuses of Valsalva can be distinguished. The left coronary artery is usually well visualized, arising at the left sinus of Valsalva to the right side of the screen. By carefully turning the probe to the left, the left coronary artery can be tracked down its course. The bifurcation can be visualized, where the left circumflex artery (LCx) runs up on the screen and the left anterior descending artery (LAD) runs down to the right side of the screen[29-31]. The right coronary artery, arising from the right sinus of Valsalva and typically running downwards on the screen, can be more difficult to image due to its smaller size and potential acoustic shadowing caused by the AV[31,32].

Measurements to be made at the root include the maximum diameters of the aortic annulus (at the hinge points of the aortic leaflets), sinus of Valsalva, and the sinotubular junction [Figure 2].

Compared to 2D TEE, the use of 3D TEE can lead to more accurate measurements of the aortic root structures. Foreshortening can be avoided by adjusting the perpendicular sectional planes[33]. Moreover, automated software combined with 3D TEE can result in accurate models and reproducible measurements of aortic root dimensions[34].

*Ascending aorta*

Compared to the aortic root, the ascending aorta runs steeper. It is best assessed from the ME AV LAX view by retracting the probe while reducing the probe angle to 90-100°[12]. The SAX view of the ascending aorta can be visualized by further reducing the probe angle to 0-10°. The proximal ascending aorta can usually be well-imaged with TEE. The right mainstem bronchus runs between the esophagus and the distal ascending aorta, which leads to refraction of the ultrasound. This area is called the blind spot [Figure 1], given that the distal ascending aorta is visible in only 10% of the cases[35]. For better visualization of this area with TEE, an endobronchial fluid-filled balloon catheter device (A-view® Cordatec Inc., Zoersel, Belgium) has been developed. With this device, the authors were able to visualize the distal ascending aorta in all cases in their study[35,36].

Epi-aortic ultrasound serves as an intra-operative alternative for TEE for visualization of the ascending aorta. With this technique, the surgeon scans the aorta via direct contact between the outer layer of the aorta and a high-frequency phased or linear probe[37].

*Aortic arch*

The aortic arch is visualized using the upper-esophageal (UE) SAX (70-90°), and the UE LAX view (0-10°)[12]. The proximal aortic arch and the brachiocephalic artery lay in the blind spot and may be difficult

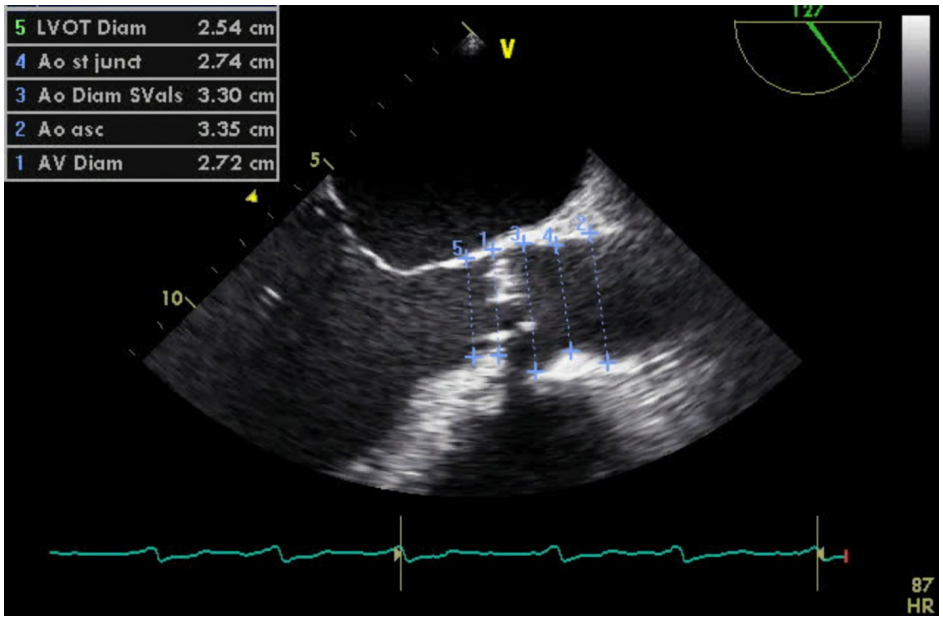


**Figure 2.** Mid-esophageal aortic valve long axis view (127) with measurements made from leading-to-leading edge. Ao: Aorta; Asc: ascendens; Diam: diameter; LVOT: left ventricular outflow tract; ST junct: sinotubular junction; SVals: sinus of valsalva.

to visualize. In one study, the origin of the brachiocephalic artery was visualized in only 36% of the subjects[38]. Similar to its application in visualizing the distal ascending aorta, the A-view® method can also be used for imaging the proximal aortic arch[35,36].

The brachiocephalic artery might be visualized starting at the aortic arch by turning the probe clockwise, withdrawing slightly, and tilting the probe to the left or right to possibly overcome the interference of the trachea[39]. Further withdrawing the probe will demonstrate the bifurcation to the right subclavian artery and the right common carotid artery[38,39].

The distal aortic arch lies close to the esophagus and can thus be well visualized with TEE. The left common carotid artery is visualized in SAX by starting from the aortic arch LAX view (0-10°) and retracting the probe with a slight counterclockwise rotation[31]. Increasing the probe angle to 90° results in imaging the carotid artery in LAX. Tilting the probe slightly to the left might evade reverberations from the trachea[38]. Starting from the UE aortic arch LAX view (0-10°), the left subclavian artery can be viewed by withdrawing the probe while counterclockwise turning, with a slight upward flexion. By retracting the probe further and turning the probe slightly counterclockwise, it is possible to image the subclavian artery in LAX, along with the origins of the vertebral artery and the left internal mammary artery (LIMA)[31,38,40].

*Descending thoracic aorta*

The descending thoracic aorta runs parallel and close to the esophagus, resulting in excellent imaging quality. It is best visualized using the descending aorta views in SAX (0-10°) and LAX (90-100°)[12]. The intercostal arteries, which arise from the descending aorta, can be visualized in short axis by slowly advancing or retracting the probe with a slight angle. The use of Color flow Doppler (CFD) can help visualize the small arteries[41]. When imaging the descending thoracic aorta in LAX, multiple intercostal arteries may be seen in the same view[12,31]. Pulsed wave Doppler (PWD) of an intercostal artery typically shows a high resistance flow pattern with a prominent anterograde systolic flow and nearly no diastolic flow. This can distinguish the intercostal arteries from other vessels such as bronchial arteries or abdominal

branches, which show a low resistance type of flow pattern with prominent anterograde flow in both systole and diastole. Veins, on the other hand, typically show a continuous blood flow in systole and diastole[41]. Left-sided pleural effusion, if present, can be seen in SAX as a dark, triangle-shaped collection next to the aorta known as the tiger's claw sign[42,43].

### Measurement of dimensions

When assessing the size of the aorta, it is essential to measure accurately and to use standardized techniques, as these measurements guide the decision for surgery[17]. By convention, aortic diameters should be obtained from leading-to-leading edge as this method gives the best correlation with measurements done with inner-to-inner edge measured by CT-scan or MRI[44]. Moreover, it is the most used technique in guidelines and reference articles[11,45]. For the best reproducibility, the aortic diameters should be measured in end diastole, since the aortic diameter has a variable increase in systole depending on the cardiac output[11,17,18,44-46].

Off-axis imaging should be avoided as it underestimates the size of the aorta in LAX views and, conversely, overestimates the size of the aorta in SAX. We recommend using simultaneous bi-plane mode to image the tubular part of the aorta from two perpendicular angles at the same time. This can help to prevent off-axis imaging as the diameter is measured perpendicular to the LAX of the aorta[11].

It is noteworthy that on ultrasound, the aortic wall thickness is falsely increased by 2 mm due to reduced axial resolution compared to CT or MRI, where the normal aortic wall thickness is typically 0.8-1.1 mm[44].

## TEE DURING SURGERY OF THE AORTA

When assessing the thoracic aorta with TEE before and during surgery, it is important to use a systematic approach. When visualizing the aortic root and ascending aorta, it makes sense to use the AV as a landmark and retract the probe slightly. When the TEE probe is turned counterclockwise to posterior, the descending aorta is usually well visualized. Retracting the probe slowly will reveal the aortic arch and its branches. A summary of the standard views that can be used to visualize the aorta in SAX and LAX is shown in Figure 1.

Prior to surgery, but particularly before initiating cardiopulmonary bypass (CPB), it is essential to conduct a comprehensive examination of the heart to detect or rule out any abnormalities. Several aortic pathologies are associated with structural heart abnormalities, i.e., aortic dilatation, dissection, coarctation, and endocarditis are linked to a bicuspid aortic valve[47]. Furthermore, aortic pathologies, particularly if the aortic root is involved, can lead to coronary dysfunction, regional wall motion abnormalities, pericardial effusion, and aortic valve regurgitation.

After weaning from CPB, the result of the surgical repair and cardiac function have to be assessed carefully and discussed with the surgeon. Surgical interventions and prolonged CPB may lead to cardiac complications such as coronary occlusion and ventricular dysfunction.

Various surgical procedures potentially lead to distinct complications. During aortic root replacement, coronary arteries are re-implanted. TEE with CFD can play a vital role by verifying blood flow in the coronary arteries and excluding the presence of new regional wall motion abnormalities. If a valve-sparing technique is used, close inspection of the aortic valve is essential. This inspection should include measurements of the coaptation length, coaptation height, mean pressure gradient, and the presence of residual regurgitation, along with the mechanism of regurgitation[48]. After AV replacement, the mean gradient over the prosthetic valve should be determined to rule out patient-prosthesis mismatch.

After ascending aorta or aortic arch replacement, the aortic lumen and the aortic branches can be visualized to assess adequate blood flow. If, during aortic arch replacement, a so-called (frozen) Elephant Trunk is placed, TEE can evaluate the position and blood flow over the Elephant Trunk[49] [Figure 3]. Elephant Trunk kinking is a rare complication, resulting in reduced blood flow in the descending aorta[50,51].

## TEE and specific aortic diseases

*Atherosclerosis*

Atherosclerosis is the most common aortic disease and is characterized by the accumulation of lipids, inflammatory cells, and connective tissue within the arterial wall. It leads to thickening of the intima and may progress to the formation of atherosclerotic plaques[17,18]. The incidence of atherosclerotic plaques increases in the course of aorta, being lowest in the ascending aorta and highest in the descending aorta[52].

Several classification systems have been proposed for grading the severity of aortic atheroma. Based on the results of most studies, atherosclerosis severity depends on the level of intimal thickening. It is considered mild with 2-3 mm (grade 1), moderate < 4 mm (grade II), severe  4 mm (grade III), and complex, when any grade is associated with mobile or ulcerated components (grade IV)[17,53,54]. Progression of the atherosclerotic plaques can lead to a penetrating aortic ulcer or aortic dissection.

The presence of aortic atherosclerosis is associated with perioperative stroke. The risk of stroke rises with increased severity of atherosclerosis, especially in the presence of protruding atheroma ≥ 4 mm, the presence of a mobile component (mural thrombosis), and if the atherosclerotic plaques are located in the ascending aorta or aortic arch[52-55]. We recommend scanning the aorta prior to incision, but particularly before cannulation and cross-clamping to identify any atherosclerotic plaques. Their presence may prompt a change in surgical strategy[56].

On TEE, aortic atherosclerosis is characterized as intimal thickening with an irregular border, often with reverberation artefacts known as comet-artefact due to aortic wall calcifications [Figure 4]. Compared to two-dimensional (2D) imaging, 3D TEE provides superior visualization of the number, morphology, volume, and spatial extent of aortic atherosclerosis[54]. Furthermore, the use of simultaneous multiplane imaging (bi-plane) can lead to more rapid imaging of atherosclerotic plaques, especially in cases with complex plaque formation[57].

Epi-aortic ultrasound may be considered in cases where atherosclerosis is suspected but the cannulation site cannot be visualized with TEE. EUS guidance on surgical manipulation can lead to a change in cannulation or aortic clamping strategy in up to 36% of the cases and may reduce the incidence of postoperative stroke[58-60] .

*Aortic dilatation and aneurysm*

Aortic dilatation is defined as an enlargement of the diameter of the aorta to more than two standard deviations from the mean predicted diameter[17]. An aneurysm is defined as an artery dilated more than 50% of the normal diameter. While this applies well for the descending thoracic aorta, it is noteworthy that for the ascending aorta and aortic arch, the risk of rupture increases before this limit is reached[61]. Therefore, several authors recommend to use the term aneurysm for diameters > 45 mm[17,62].

The most common site of thoracic aortic aneurysm is the aortic root and ascending aorta (60%), followed by the descending aorta (35%) and the aortic arch (< 10%)[62]. Approximately 20% of the thoracic aortic aneurysms are related to a genetic disorder, such as Marfan's syndrome or Ehler Danlos[63].

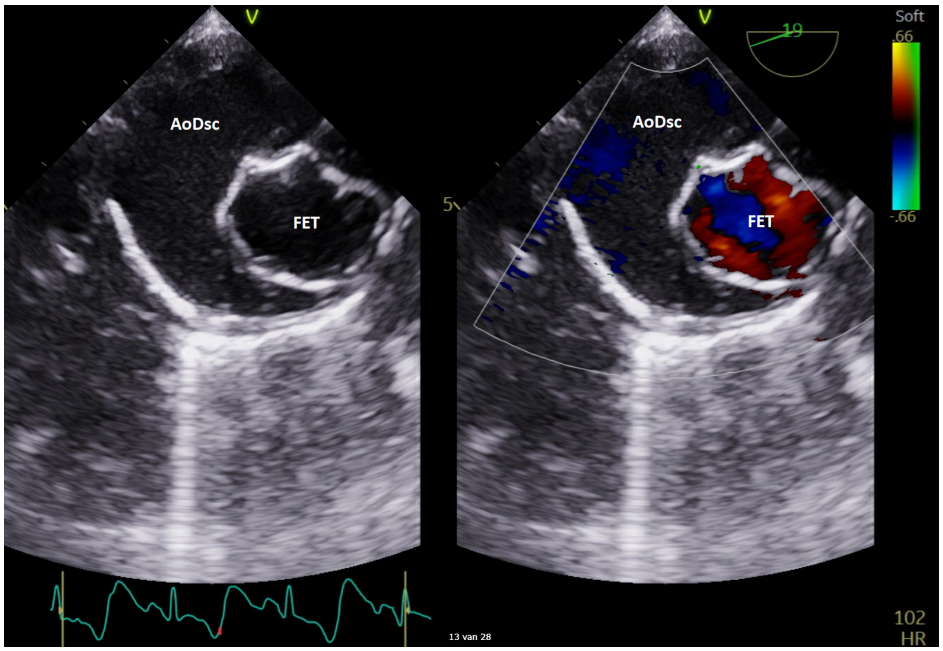


**Figure 3.** Descending aorta short axis view. An enlarged descending aorta can be seen, with the Frozen Elephant Trunk clearly visible in the lumen. Right image with color flow Doppler with adequate flow in the Frozen Elephant Trunk. AoDs: Descending aorta; FET: frozen elephant trunk.

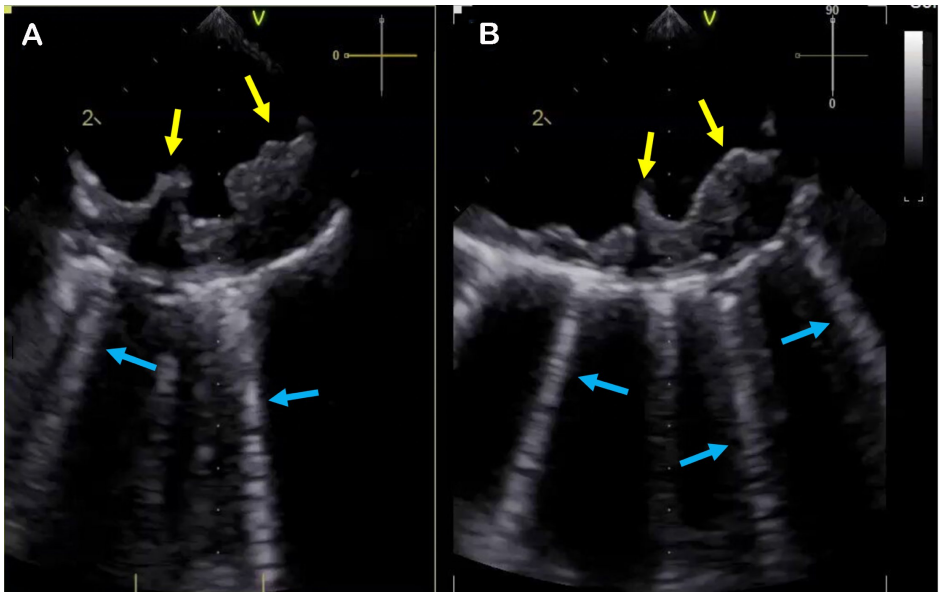


**Figure 4.** Simultaneous multiplane image with (A) Mid-esophageal descending aorta short axis view (0) and (B) Mid-esophageal descending aorta long axis view (90). Yellow arrows: Severe atherosclerosis (grade IV) with intimal thickening > 10 mm and irregular border. Blue arrows: Multiple reverberation artefacts from the calcified aortic (comet-tails).

Preoperatively, it is important to document the size and location of the aneurysm with TEE, although it can be challenging to measure the exact diameter of the dilated aorta due to off-axis imaging. Aortic regurgitation (AR) is a common secondary complication of aortic root and ascending aorta dilatation and can be severe[64]. When present, the severity and etiology of AR should be assessed with TEE.

Sinus of Valsalva aneurysm is a rare congenital or acquired defect, which leads to severe dilatation of one or more sinuses. It can lead to rupture of nearby structures, in most cases, the right ventricle or the right atrium. In the event of rupture, CFD shows a continuous positive flow from the aorta to the nearby structure in both systole and diastole[65].

*Aortic dissection*

Aortic dissection (AD) is a result of a disruption of the intima (tear), leading to the accumulation of blood between the intima and media. This results in the formation of a second lumen, the so-called false lumen. Intimal tears typically occur at points of greatest wall stress, most commonly just above the sinotubular junction on the greater curve or just distal to the origin of the left subclavian artery. AD can be classified anatomically according to Stanford or DeBakey. AD is classified as Stanford type A or DeBakey I/II if the ascending aorta is dissected regardless of the location of the intimal tear. If the dissection is limited to the descending aorta, AD is classified as Stanford type B or DeBakey III. If the aortic arch is involved but not the ascending aorta, AD is classified as non-A-non-B[66,67]. The indication of surgical treatment depends on the type of dissection; Stanford type A and non-A-non-B AD usually require (immediate) surgery.

TEE can be used as a diagnostic modality for AD, with sensitivity reaching up to 99% and specificity 89% in acute cases[17]. The diagnosis of chronic AD can be more difficult to make with TEE, especially in cases where false lumen is completely thrombosed[55].

The intimal flap, which separates the true and false lumen, appears on TEE as a mobile echodense line[11,68]. An example of a dissection flap visualized on TEE is shown in Figures 5 and 6. The entry or re-entry tears appear as a disruption of the intimal flap and CFD shows blood flow over the tear. Imaging artefacts such as reverberation artefacts or side lobe artefacts can give a false impression of AD. Therefore, it is important to obtain multiple images of the intimal flap in different views[11,17,68].

Preoperatively, the proximal extension of the intimal flap should be demonstrated precisely to guide surgical decision making for aortic reconstruction. If possible, the distal extension of AD should be demonstrated as well. Studies indicate that the use of 3D TEE improves the location and size of the entry tear compared to 2D echocardiography[69]. Furthermore, 3D TEE has been shown to enhance the visualization of the extent of the dissection flap[70].

After visualizing the dissection flap, it is essential to differentiate the true and the false lumen[11]. Important criteria include:

The false lumen is most often larger than the true lumen, especially further distal in the aortic arch and descending aorta.

PWD displays higher blood flow velocities in the true lumen in systole compared to the false lumen[11]. Low blood flow velocities can be displayed as spontaneous echo contrast or thrombosis in the false lumen.The true lumen expands in systole, while the false lumen is compressed. M-mode can help to visualize the extension and compression.

At the entry tear, CFD displays blood flow from true to false lumen in systole.

The direction of flow is anterograde in the true lumen, whereas it can be retrograde in the false lumen.

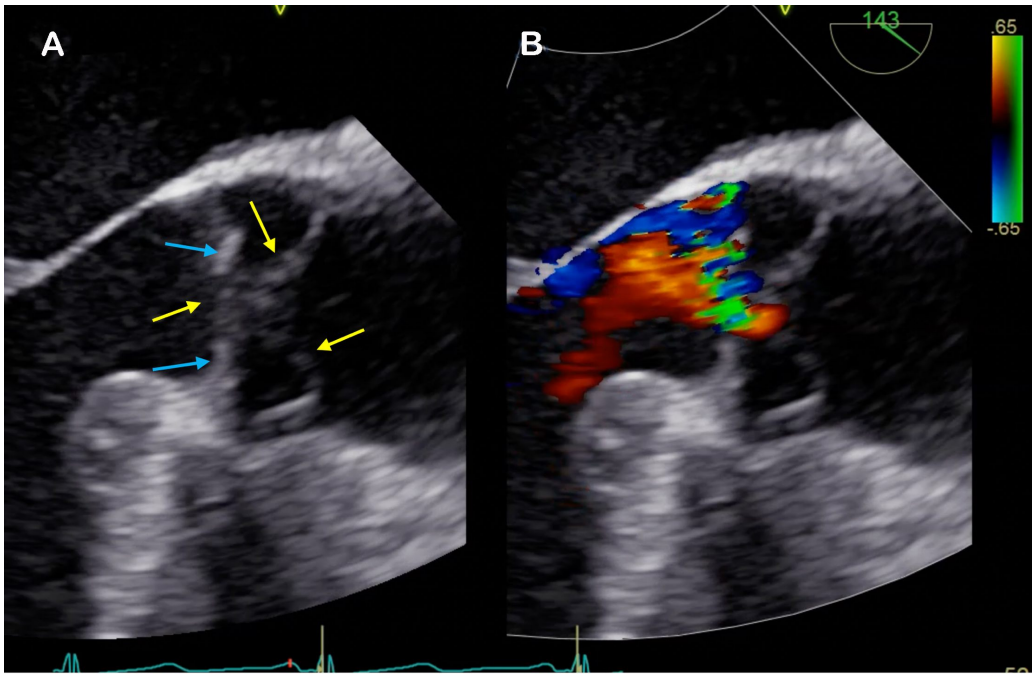


**Figure 5.** Mid-esophageal aortic valve long-axis view (143) in a patient with type A aortic dissection. (A) The dissection flap (yellow arrows) is seen passing through the aortic valve (blue arrows) in end-diastole. (B) The same image with color flow Doppler, showing moderate aortic regurgitation.

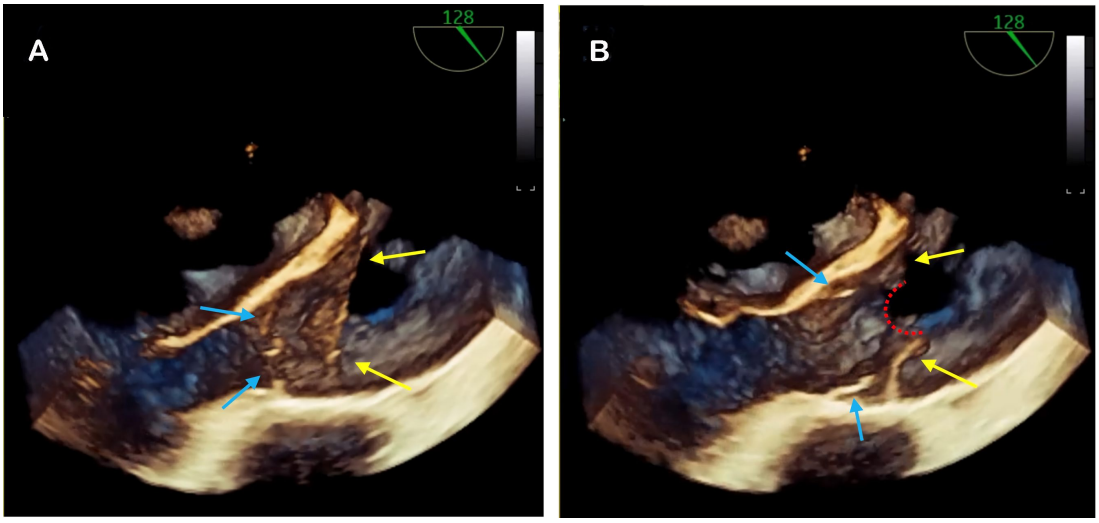


**Figure 6.** Three-dimensional imaging of the mid-esophageal aortic valve long axis view (128) in a patient with type A aortic dissection. (A) In mid-diastole, the aortic valve (blue arrows) and dissections flap (yellow arrows) are seen. (B) In systole, the aortic valve opens (blue arrows) and the dissection flap (yellow arrows) is moved forward, showing the entry tear (red line).

The differentiation of the true and false lumen is particularly important for cannulation strategies. In cases where a guidewire is used, also known as Seldinger aortic cannulation, it is essential to confirm the position of the guidewire in the true lumen and to ensure it stays in place during the cannulation procedure. In alternative cannulation strategies, such as direct true lumen cannulation or the "Samurai procedure", TEE can be used to visualize the correction of flow in the true lumen and exclude true lumen collapse after initiation of CPB[71].

Further comprehensive imaging should determine the presence of associated complications due to AD, such as pericardial effusion, coronary artery or aortic branch involvement and para-aortic fluid[11,72]. Aortic regurgitation (AR) is the most frequent associated complication, and might result from dilatation of the aortic root, prolapse of the dissection flap through the AV or detachment of the valve commissures due to the dissection itself[66].

The etiology and classification of aortic regurgitation should be assessed preoperatively, as this guides the surgical decision process[73]. Type 1a AR, as a result of STJ and ascending aorta enlargement, will typically be corrected by restoring the geometry of STJ and ascending aorta. Type 1b, due to the extension of the dissection into the aortic root, can be managed by aortic root repair or replacement. Type II AR may be a result of aortic cusp prolapse due to commissural disruption or AV detachment, and can be surgically managed by aortic valve repair or replacement. Finally, Type III AR may be caused by intimal flap passage through the valve, which requires resection of the intimal flap[64,73].

Figure 5 shows an example of a dissection flap passing through the aortic valve.

After surgery, the evaluation of the repair with TEE includes aortic valve function, coronary flow detection, and regional wall motion abnormalities. The flow in the aortic lumens should be assessed by the echocardiographist to determine the correct flow in the true lumen and to rule out a residual connection between the true and false lumen.

*Intramural hematoma*

An intramural hematoma (IMH) occurs when blood collects in the media of the aortic wall, with the absence of an intimal tear, resulting from media *vasa vasorum* hemorrhage or rupture of an atherosclerotic plaque[18,68,74].

Typically, an intramural hematoma appears as a thickening of the aortic wall > 5 mm in a crescent-shape or concentric pattern. In patients with severe atherosclerosis, a cut-off value of > 7 mm is more specific[17]. The aortic wall shows a mixed echogenicity with predominant echo densities and no detectable blood flow[18,68,74]. The aortic lumen shape is generally preserved. The luminal wall is curvilinear and usually smooth [Figure 7]. This differentiates IMH from aortic atherosclerosis and intraluminal thrombus that presents more frequently with a rough, irregular surface[17,18,20,74]. Compared to AD, IMH is generally a more localized process, whereas a (thrombosed) false lumen often has a spiral course and shows an irregular intimal surface[17,74]. On the other hand, the extension of an IMH to the aortic lumen may eventually result in AD.

*Iatrogenic aortic lesions*

Iatrogenic aortic dissection (IAD) can result from several procedures such as coronary angiography, cardiac surgery, endovascular aortic procedures, intra-aortic balloon pump, or transcatheter aortic valve replacement[75]. During cardiac surgery, IAD occurs most frequently on the site of aortic arterial cannulation, on the site of aorta cross-clamping, and on the venous graft anastomosis[18,75] [Figure 8]. TEE can play a crucial role in readily confirming the diagnosis, when IAD is suspected by demonstrating an intimal flap and, if possible, the intimal tear. Besides confirming the diagnoses, TEE can be used to investigate the extension of injury and to detect any associated complications.

The mortality of IAD is more than doubled when it is diagnosed in the early postoperative period compared to the intraoperative period[76]. Therefore, we recommend routinely inspecting the aortic arch and descending aorta with TEE after surgery to detect or rule out IAD.

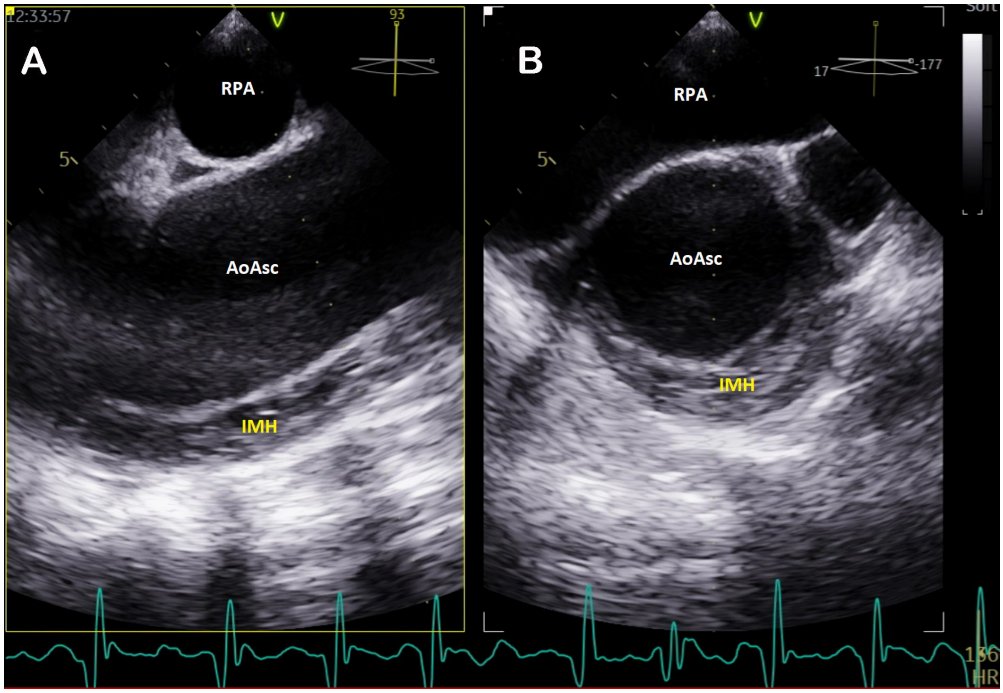


**Figure 7.** Simultaneous bi-plane image. (A) Mid esophageal ascending aorta long axis (93°). (B) Mid esophageal ascending aorta short axis (17°). An intramural hematoma is seen in the ascending aortic wall. AoAsc: Ascending aorta; IMH: intramural hematoma; RPA: right pulmonary artery.

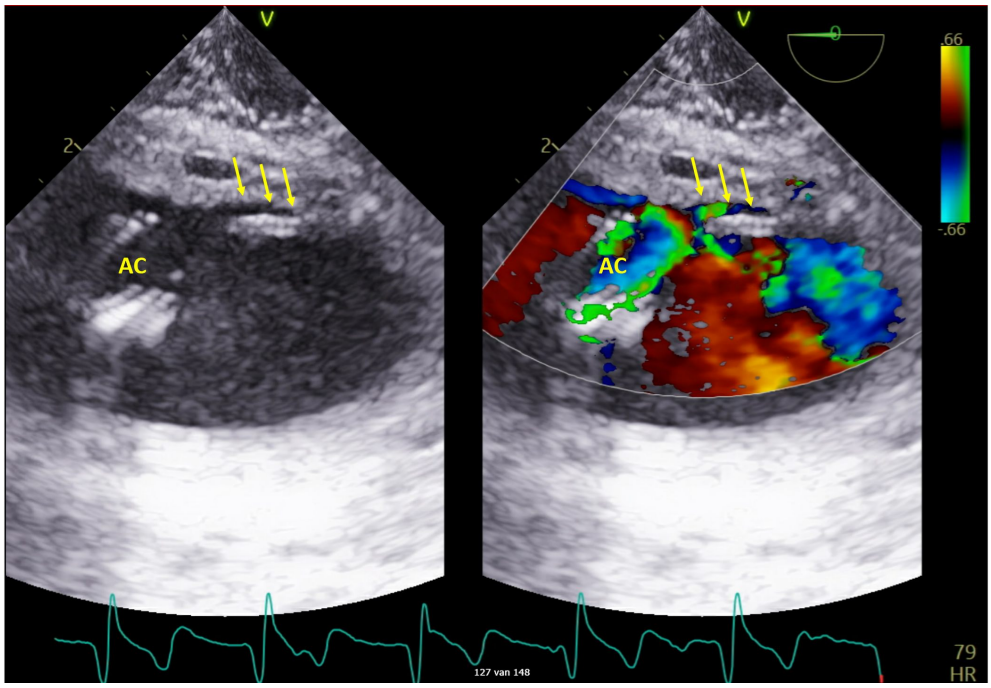


**Figure 8.** Upper aortic arch IAX view. Right image with color flow Doppler. Canula is visible in aortic arch (AC). Iatrogenic Aortic Dissection can be seen (yellow arrows).

Iatrogenic intramural hematoma is a rare complication and has been described in literature in some case reports. In the perioperative setting, it can be caused by placement or manipulation of the aortic cannulas or by aortic cross-clamping[77]. Furthermore, it has been described to be caused by retrograde coronary dissection into the aortic root during percutaneous coronary interventions[78]. The echocardiographic assessment of iatrogenic IMH is similar to spontaneous IMH. It can be challenging to distinguish iatrogenic IMH from IAD[78,79].

*Penetrating aortic ulcer*

A penetrating aortic ulcer (PAU) occurs when an aortic atherosclerotic plaque ulcerates through the intima into the media of the aortic wall. It occurs predominantly in the descending aorta and less frequently in the aortic arch[18]. PAU can lead to an intramural hematoma, AD, aortic aneurysm, or rupture, if the adventitia is affected[68]. PAU appears on TEE as a focal, outpouching lesion with a rough, serrated edge[68,74] [Figure 9]. In the acute phase, it is frequently accompanied by hematoma localized around the lesion[74].

*Traumatic aortic injury/aortic rupture*

Traumatic aortic injury (TAI) most often occurs in blunt trauma or deceleration injuries. It can result in a variety of lesions, including AD, IMH, (pseudo)aneurysm formation, or (contained) rupture[18,62,80].

Aortic rupture is characterized as a disruption of all the aortic wall layers, leading to an acute, devastating clinical presentation that requires emergent repair whenever possible. Contained rupture commonly manifests as an aortic pseudoaneurysm, defined as a dilatation of the aorta due to disruption of all wall layers, which is only contained by the periaortic connective tissue[17,80].

The most common location of traumatic aortic injury is at the aortic isthmus just distal to the left subclavian artery, followed by the supravalvular portion of the ascending aorta. This is a result of torsion and shearing stress, while these structures are relativly immobile[18,62,80]. For TEE during surgery, it is important to visualize the aorta as much as possible to rule out any undetected lesions. TAI is frequently accompanied by mediastinal hematoma[80].

*Aortic coarctation*

Aortic coarctation is characterized as a narrowing of the aortic lumen due to a ridge of dense tissue. It is most often located just distal to the left subclavian artery, where the former ductus arteriosus was situated[81]. Aortic coarctation is typically congenital, although it can have an acquired cause due to inflammatory diseases or severe atherosclerosis[82]. Severe stenosis is suggested by high-velocity flow on CFD with continuous systolic and diastolic forward flow. Doppler gradient measurements are often unreliable because of the inadequate alignment of the ultrasound beam[81,83]. Post-stenotic dilatation of the descending aorta may be observed. Structural lesions associated with aortic coarctation and detectable with TEE are bicuspid aortic valve, left heart inflow and outflow anomalies, ventricular septum defects, and patency of the ductus arteriosus.

TEE can differentiate aortic coarctation from other aortic arch anomalies, such as pseudocoarctation and aortic arch hypoplasia. In pseudocoarctation, a marked dilatation of the aorta and kinking of the proximal descending aorta can be seen on ultrasound. Aortic arch hypoplasia, although rarely discovered in adults, is characterized by incompletely developed, narrowed arch with acute angulation[84].

*Infectious endocarditis*

Infectious endocarditis (IE) is a severe disease affecting heart tissue and valves and is associated with high

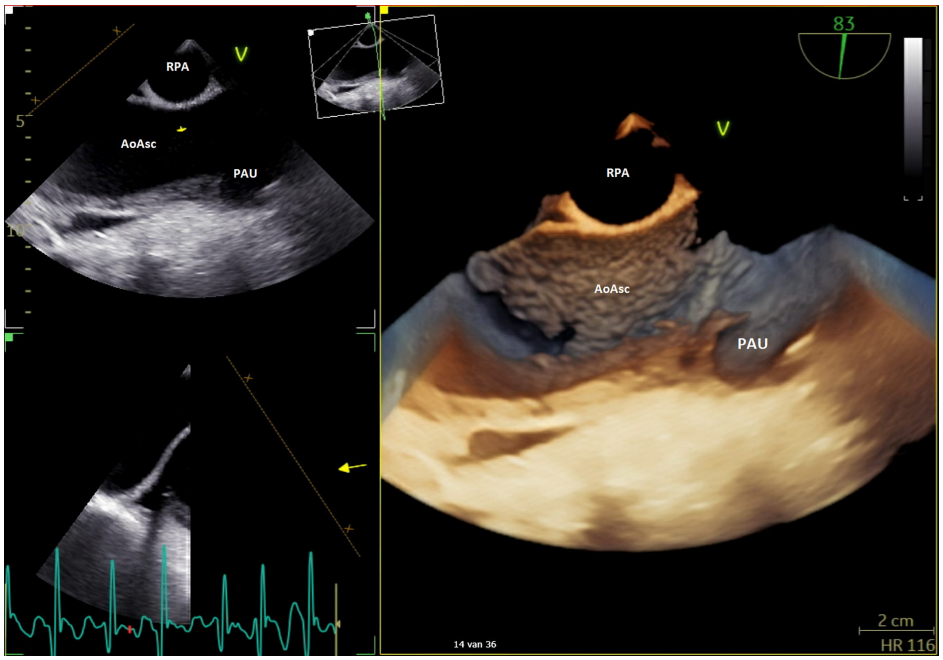


**Figure 9.** 2D (left upper) and 3D (right) image of the ascending aorta. A penetrating aortic ulcer can be seen. AoAsc: Ascending aorta; PAU: penetrating aortic ulcer; RPA: right pulmonary artery.

morbidity and mortality. The extent of IE can vary and it is characterized anatomically by a combination of vegetations, destructive valve lesions, and, in severe cases, abscess formation[85]. TEE plays a key role in the diagnosis of endocarditis in the preoperative period and it is used for prognostic assessment, risk stratification, and surgical decision and timing[86]. The risk of embolization is significantly increased with large (more than 10 mm) and highly mobile vegetations, or located on the mitral valve, as demonstrated by echocardiography[87-90]. Especially 3D TEE is useful for the evaluation of the size and morphology of vegetations, as it results in more accurate measurements than 2D TEE[91].

IE can result in aortic root abscess, which can be visualized on echocardiography as a nonhomogeneous echolucent, occasionally echodense area [Figure 10]. By definition, there is no connection between the abscess and the adjacent blood pool. If the abscess drains into the aortic lumen, it leads to the formation of a pseudoaneurysm, characterized by pulsatile flow on CFD[92]. Further progression of IE may lead to fistula from the aorta to the nearby heart chambers, visualized on TEE by highly turbulent systolic and diastolic flow across the fistula[92,93].

In the perioperative period, TEE is essential to assess the extent and the exact location of the infectious lesions before initiation of CPB, as the results of TEE often change the operative plan[92,94]. After weaning of CPB, a TEE study is essential to evaluate the surgical treatment and to decide whether further surgical interventions are needed[94]. If IE is related to a prosthetic aortic valve or Bentall graft infection, TEE might not be conclusive due to artifacts of the prosthetic valve[75].

*Aortic graft infection*

Aortic graft infection is a rare, but devastating complication after surgical or endovascular treatment of aortic pathologies. It normally indicates surgical intervention with significant early morbidity and mortality[95]. Surgical treatment options consist of partial or complete removal of the graft or debridement and irrigation[96].

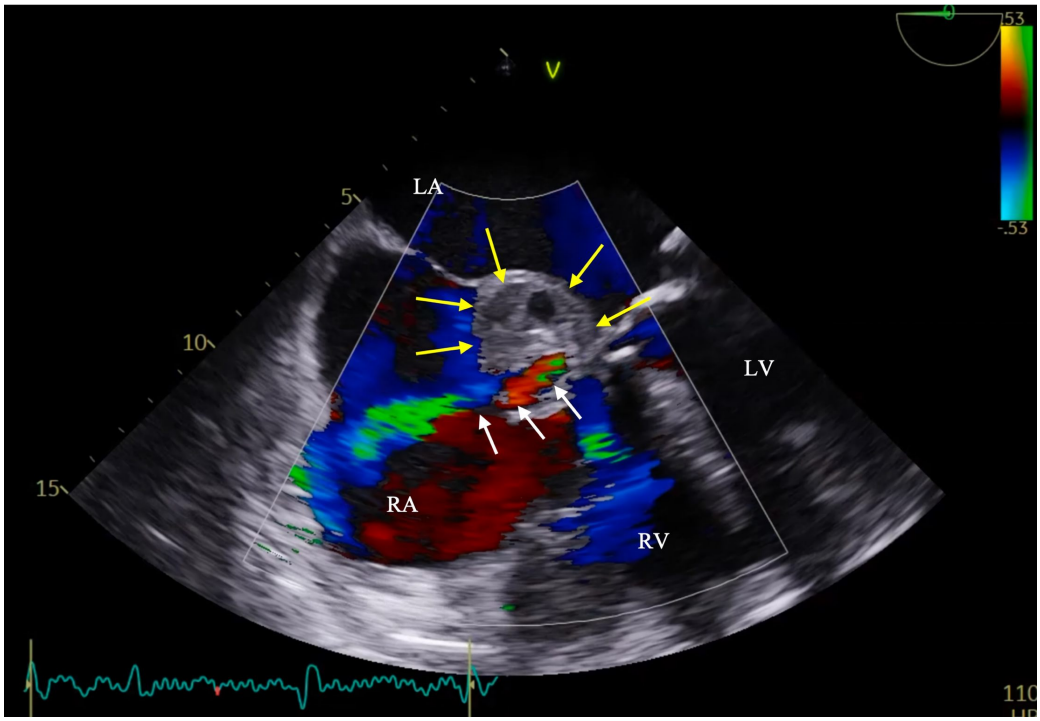


**Figure 10.** Modified mid-esophageal five-chamber view (0) with a focus on the right atrium. A large aortic root abscess presents (yellow arrows) with a fistula (white arrows) from the aortic root to the dilated right atrium. Continuous flow in systole and diastole is seen using color flow Doppler. LA: Left atrium; LV: left ventricle; RA: right atrium; RV: right ventricle.

On TEE, the infected graft may appear thickened and para-aortic fluid collections, hematoma, or abscesses may be seen[97]. Other findings on echocardiography associated with aortic graft infection include graft anastomotic disruption, fistulae, vegetations, or aneurysm formation[95].

Graft infections of the ascending aorta, in combination with prosthetic valve infection, may lead to valvular dysfunction or valvular dehiscence.

## TEE FOR ENDOVASCULAR SURGERY ON THE AORTA

Thoracic endovascular aortic repair (TEVAR) has been used for two decades and has revolutionized the treatment for disease of the aorta. It is now the preferred approach for the treatment of aneurysms of the descending thoracic aorta, due to its reduced morbidity, hospital length of stay, and short-term mortality compared to open thoracic aneurysm repair[98]. Although TEVAR was developed for the treatment of aneurysmal disease, treatment indications now include complicated type B aortic dissection, intramural hematoma, penetrating aortic ulcer, and traumatic aortic lesions[98,99]. Recently, developments have been made for endovascular ascending aortic and aortic arch repair. This may be an alternative for patients who are considered at increased risk for open surgery[100].

Besides visualizing aortic pathologies as described previously, TEE can be used for the surgical guidance of several specific aspects of endovascular procedures:

Endovascular aortic surgery is performed using guidewires, which are usually placed retrograde via the femoral arteries. Correct positioning can be confirmed by TEE by demonstrating the guidewire in the

descending aorta in the descending aorta SAX (0-10°). The guidewire will show up as a small, echogenic dot in the lumen. If the guidewire lies close to the aortic wall, it may be difficult to visualize. Simultaneous bi-plane mode or 3D imaging can demonstrate the guidewire in SAX and LAX, which aids in the visualization and can exclude potential artifacts [Figure 11]. It is noteworthy that during endovascular repair of the ascending aorta, the guidewires are placed across the aortic valve into the ventricular lumen.

In cases of AD, the standard imaging modalities used during TEVAR (fluoroscopy and angiography) cannot directly verify the correct positioning in the true lumen. However, with TEE, the true lumen can be identified and correct guidewire positioning can readily be confirmed[101,102]. Figure 12 shows an example of confirmation with TEE of the correct placement of a guidewire in the descending aorta.

During the procedure, TEE is suited as an imaging modality in addition to fluoroscopy and angiography for the guidance of the stent positioning. The presence of atherosclerotic plaque may complicate correct stent placement, and scanning the aorta on the site of stent deployment may detect or rule out its presence[103]. Ideally, stent grafts require a 20-25 mm landing zone proximal and distal to the lesion to acquire an adequate seal[99,104,105]. This landing zone can be determined by TEE. Subsequently, the tip of the probe can be set facing the most ideal landing zone, serving as a reference point for fluoroscopy[101,103]. For endovascular ascending aorta repair, the determination of the landing zone can be challenging and smaller distances may be accepted. The most common site for the entry tear in AD is just distal to the sinotubular junction, and in these cases, the sinotubular junction has been used as the proximal landing zone in several cases[104,106]. Even more proximal placement of the stent graft within the sinus of Valsalva has been described[104,107]. While visualizing the aorta in LAX, the correct stent graft positioning can be confirmed before and during stent graft deployment [Figure 13].

In TEVAR after aortic arch replacement with (Frozen) Elephant Trunk, TOE can be used to confirm the correct placement of guidewires and the endovascular stent in the Elephant Trunk, especially in challenging cases. The same applies to the positioning of an endo-prosthesis for the extension of a previous TEVAR. Moreover, recently developed hybrid grafts for thoracoabdominal aortic repair, such as the Toracoflo® (Terumo, Tokyo, Japan), rely completely on intraoperative TEE for the correct positioning of the endovascular part of the hybrid graft[108,109].

After stent deployment, the echocardiographist should confirm correct positioning and search for gross endoleaks. In addition, TEE can be used to detect flow in the stent graft excluded zone, the aneurysmal or false lumen. Exclusion from the blood pool leads to an initial "smoke phenomenon", caused by initial thrombosis in this lumen. This can serve as a confirmation that the aneurysm or the primary entry is correctly stented[101,103]. CFD with the Nyquist limit reduced to 25 cm/s can be used to detect residual flow in the aneurysmal or false lumen[101]. Anterograde flow in the aneurysmal or false lumen indicates endoleak, while retrograde flow suggests flow from a re-entry tear. These findings may indicate extra stent graft placement or additional balloon dilatation. Studies have shown that the findings on TEE contributed to an alternation of the procedures in 38%-59% of cases[101,102].

After the procedure, TEE can be used to detect any new lesions, such as intimal tears proximal or distal from the stent graft. Furthermore, if the distance between the stent graft and aortic branches and the stent is small, TEE can be used to confirm adequate flow in these branches after stent deployment[101]. In ascending aorta stent grafting, TEE can be used to detect or rule out several specific complications. The AV could be damaged from stiff guidewire placement near or across the valve. Therefore, it should be evaluated for structural changes and functional abnormalities such as (worsening of) aortic regurgitation. Entrapment of

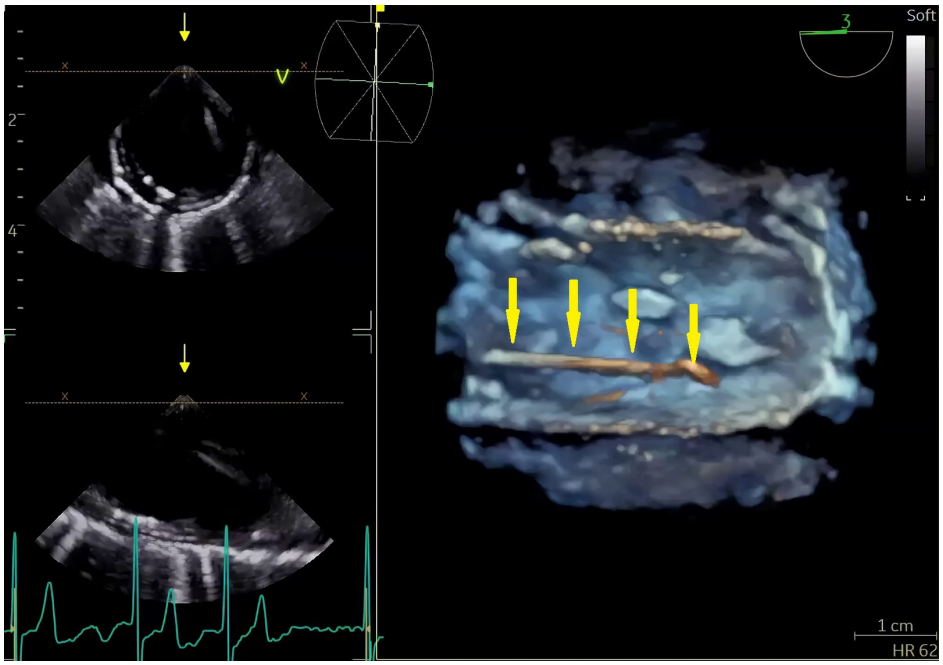


**Figure 11.** Three-dimensional view of a guidewire (yellow arrows) with correct placement in the descending aorta.

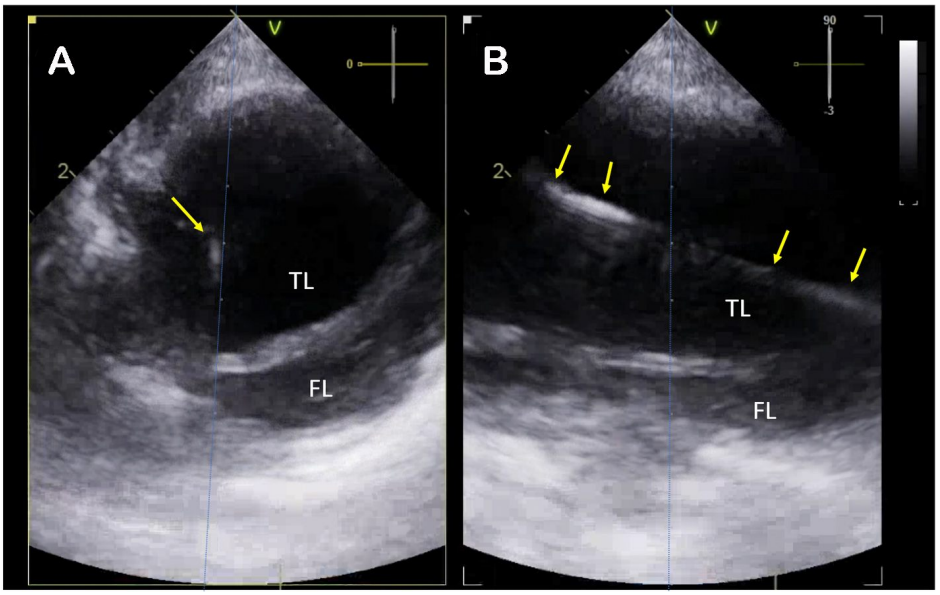


**Figure 12.** Simultaneous bi-plane image of the descending aorta with aortic dissection. (A) Descending aorta short axis 0° view. The true and false lumen can be differentiated. The guide wire can be seen as a small dot (yellow arrow). (B) Descending aorta long axis 90° view. The guidewire can be seen in long axis (yellow arrows). Note that in this case, the true lumen was larger than the false lumen. FL: False lumen; TL: true lumen.

the guidewires in the mitral-valve subvalvular apparatus can occur. Moreover, the stent graft could potentially occlude the coronary ostia. Therefore, the coronary artery blood flow and normal regional wall motion should be confirmed.

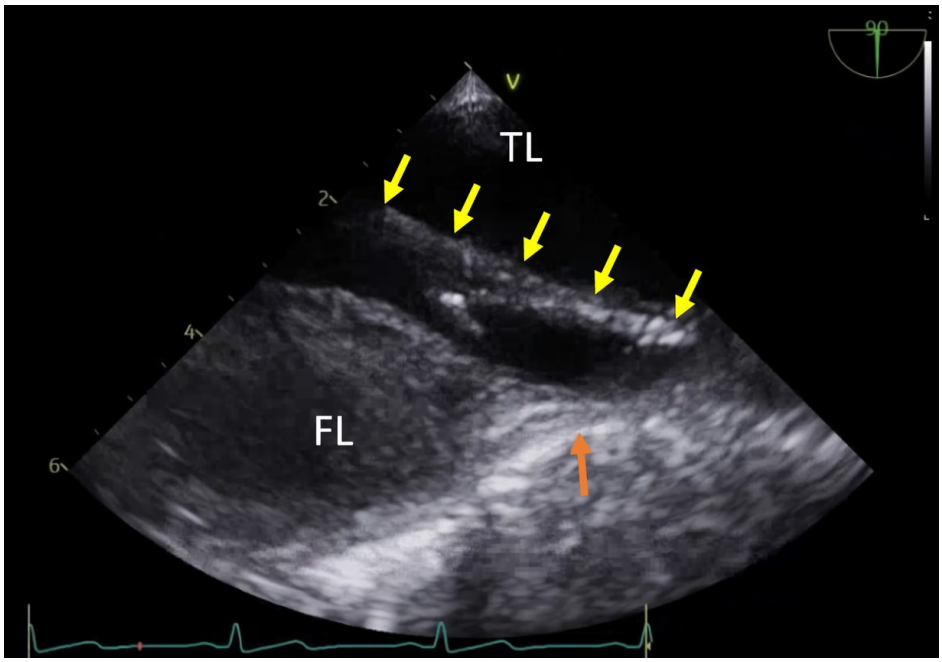


**Figure 13.** Descending aorta long axis 90° view with chronic aortic dissection, with a partially thrombosed false lumen. The proximal extent of the dissection is indicated with the upward orange arrow. The not-yet-deployed endovascular stent graft is seen (yellow arrows). FL: False lumen; TL: true lumen.

## LIMITATIONS OF PERIOPERATIVE TEE

Although of great value during the perioperative period, TEE has some important limitations. The imaging quality is highly operator-dependent. Extensive training is needed, especially for the visualization of complex structures, flow patterns, and 3D echocardiography. Patient-specific contraindications may limit the use of TEE in the perioperative setting. These contraindications include esophageal varices or strictures, or a medical history of esophageal or gastric surgery[13]. As previously described, not all segments of the thoracic aorta are well seen with TEE. Particularly, the distal ascending aorta and the proximal aortic arch can be challenging to visualize. Moreover, calcifications, artefacts, and foreign bodies such as cannulas and prosthetic valves can compromise image quality. Furthermore, the spatial imaging of the thoracic aorta faces limitations due to the narrow 90° image sector, preventing the inclusion of long segments of the aorta, which may restrict topographic orientation[17,20].

## FUTURE DIRECTIONS

Ongoing development is being made in ultrasound technology, leading to better imaging resolution, higher frame rate, and fewer artefacts. Increasing computer processing power on commercial ultrasound machines makes real-time 3D imaging with CFD more accessible in the operating theater. In addition, new imaging techniques have been developed, such as blood speckle imaging (BSI), which visualize flow patterns and blood vector velocities[110]. Current publications studying the fluid dynamics with this novel technique are mainly in the field of cardiac imaging, pediatric and congenital cardiology[111-113]. To date, no articles have yet been published concerning blood flow patterns during aortic surgery, although this may be an interesting addition to the functional evaluation of complex surgical repairs of the aorta.

Contrast-enhanced ultrasound (CEUS) has been used for cardiac imaging for decades. In this imaging modality, an intravenous contrast agent containing micro-bubbles is admitted, which aids in the imaging of

luminal borders, such as ventricular or vascular walls. In postoperative surveillance after endovascular surgery, it has been shown to be more sensitive and accurate for the detection and classification of endoleak compared to CT[114]. Furthermore, during TEVAR procedures, CEUS is feasible and more sensitive in the detection of endoleaks compared to standard TEE, making it an interesting addition to the perioperative imaging strategy for the guidance and control of TEVAR procedures[115,116].

Not surprisingly, ongoing development is made in surgical techniques and devices as well. An interesting concept is the Endo-Bentall, an endovascular device for AV and ascending aorta replacement[117]. The device consists of a transcatheter aortic valve prosthesis connected to an uncovered portion of the stent graft. The concept device is implanted via the transapical route and uses the AV annulus, sinotubular junction, and distal ascending aorta as landing zones while the uncovered portion of the stent-graft with coronary stents secures coronary perfusion[117]. To date, it has been utilized sporadically with custom-made or modified devices[118,119]. Alternatively, in one case, off-the-shelve grafts were implanted via the transarterial route[120]. Since the aortic root is a complex structure and correct positioning of the device is essential, perioperative TEE can be a valuable tool for surgical guidance and evaluation, and detection of complications. TEE has demonstrated right ventricular dysfunction due to coronary obstruction in one published case[120].

## CONCLUSION

TEE is used during surgery on the aorta for the detection of aortic pathology, guiding of surgical decision making, and evaluation of the surgical repair. For perioperative echocardiographists, it is essential to know the key elements of TEE and aortic disease, as summarized in this article. With the developments made in echocardiography and surgical techniques, TEE remains an invaluable tool in the operation theater, now and in the future.

## DECLARATIONS

### Authors' contributions

Literature search, conception, design, writing of the article: Alberts T, Eberl S, Hermanns H

### Availability of data and materials

Not applicable.

### Financial support and sponsorship

None.

### Conflicts of interest

All authors declared that there are no conflicts of interest.

### Ethical approval and consent to participate

Not applicable.

### Consent for publication

Not applicable.

## REFERENCES

1. MacKay EJ, Neuman MD, Fleisher LA, et al. Transesophageal echocardiography, mortality, and length of hospitalization after cardiac valve surgery. *J Am Soc Echocardiogr* 2020;33:756-62.e1. DOI PubMed PMC
2. MacKay EJ, Zhang B, Augoustides JG, Groeneveld PW, Desai ND. Association of intraoperative transesophageal echocardiography and clinical outcomes after open cardiac valve or proximal aortic surgery. *JAMA Netw Open* 2022;5:e2147820. DOI PubMed PMC
3. Dieleman JM, Myles PS, Bulfone L, et al. Cost-effectiveness of routine transoesophageal echocardiography during cardiac surgery: a discrete-event simulation study. *Br J Anaesth* 2020;124:136-45. DOI
4. Vegas A. Three-dimensional transesophageal echocardiography: principles and clinical applications. *Ann Card Anaesth* 2016;19:S35-43. DOI PubMed PMC
5. van Ramm OT, Smith SW. Real time volumetric ultrasound imaging system. *J Digit Imaging* 1990;3:261-6. DOI PubMed
6. Sugeng L, Shernan SK, Salgo IS, et al. Live 3-dimensional transesophageal echocardiography initial experience using the fully-sampled matrix array probe. *J Am Coll Cardiol* 2008;52:446-9. DOI
7. Purza R, Ghosh S, Walker C, et al. Transesophageal echocardiography complications in adult cardiac surgery: a retrospective cohort study. *Ann Thorac Surg* 2017;103:795-802. DOI
8. Huang CH, Lu CW, Lin TY, Cheng YJ, Wang MJ. Complications of intraoperative transesophageal echocardiography in adult cardiac surgical patients - experience of two institutions in Taiwan. *J Formos Med Assoc* 2007;106:92-5. DOI PubMed
9. Kallmeyer IJ, Collard CD, Fox JA, Body SC, Shernan SK. The safety of intraoperative transesophageal echocardiography: a case series of 7200 cardiac surgical patients. *Anesth Analg* 2001;92:1126-30. DOI PubMed
10. Patel KM, Desai RG, Trivedi K, Neuburger PJ, Krishnan S, Potestio CP. Complications of transesophageal echocardiography: a review of injuries, risk factors, and management. *J Cardiothorac Vasc Anesth* 2022;36:3292-302. DOI PubMed
11. Nicoara A, Skubas N, Ad N, et al. Guidelines for the use of transesophageal echocardiography to assist with surgical decision-making in the operating room: a surgery-based approach: from the American Society of Echocardiography in Collaboration with the Society of Cardiovascular Anesthesiologists and the Society of Thoracic Surgeons. *J Am Soc Echocardiogr* 2020;33:692-734. DOI
12. Hahn RT, Abraham T, Adams MS, et al. Guidelines for performing a comprehensive transesophageal echocardiographic examination: recommendations from the American Society of Echocardiography and the Society of Cardiovascular Anesthesiologists. *J Am Soc Echocardiogr* 2013;26:921-64. DOI
13. AmericanSociety of Anesthesiologists and Society of Cardiovascular Anesthesiologists Task Force on Transesophageal Echocardiography. Practice guidelines for perioperative transesophageal echocardiography. *Anesthesiology* 2010;112:1084-96. DOI PubMed
14. Flachskampf FA, Wouters PF, Edvardsen T, et al; European Association of Cardiovascular Imaging Document reviewers: Erwan Donal and Fausto Rigo. Recommendations for transoesophageal echocardiography: EACVI update 2014. *Eur Heart J Cardiovasc Imaging* 2014;15:353-65. DOI
15. Sievers HH, Hemmer W, Beyersdorf F, et al; Working Group for Aortic Valve Surgery of German Society of Thoracic and Cardiovascular Surgery. The everyday used nomenclature of the aortic root components: the tower of Babel? *Eur J Cardiothorac Surg* 2012;41:478-82. DOI
16. Popieluszko P, Henry BM, Sanna B, et al. A systematic review and meta-analysis of variations in branching patterns of the adult aortic arch. *J Vasc Surg* 2018;68:298-306.e10. DOI
17. Evangelista A, Sitges M, Jondeau G, et al. Multimodality imaging in thoracic aortic diseases: a clinical consensus statement from the European Association of Cardiovascular Imaging and the European Society of Cardiology Working Group on aorta and peripheral vascular diseases. *Eur Heart J Cardiovasc Imaging* 2023;24:e65-85. DOI
18. Erbel R, Aboyans V, Boileau C, et al; ESC Committee for Practice Guidelines. 2014 ESC guidelines on the diagnosis and treatment of aortic diseases: document covering acute and chronic aortic diseases of the thoracic and abdominal aorta of the adult. The task force for the diagnosis and treatment of aortic diseases of the european society of cardiology (ESC). *Eur Heart J* 2014;35:2873-926. DOI
19. Zafar MA, Li Y, Rizzo JA, et al. Height alone, rather than body surface area, suffices for risk estimation in ascending aortic aneurysm. *J Thorac Cardiovasc Surg* 2018;155:1938-50. DOI
20. Goldstein SA, Evangelista A, Abbara S, et al. Multimodality imaging of diseases of the thoracic aorta in adults: from the American Society of Echocardiography and the European Association of Cardiovascular imaging: endorsed by the society of cardiovascular computed tomography and society for cardiovascular magnetic resonance. *J Am Soc Echocardiogr* 2015;28:119-82. DOI
21. Devereux RB, de Simone G, Arnett DK, et al. Normal limits in relation to age, body size and gender of two-dimensional echocardiographic aortic root dimensions in persons ≥ 15 years of age. *Am J Cardiol* 2012;110:1189-94. DOI PubMed PMC
22. Campens L, Demulier L, De Groote K, et al. Reference values for echocardiographic assessment of the diameter of the aortic root and ascending aorta spanning all age categories. *Am J Cardiol* 2014;114:914-20. DOI
23. Davis AE, Lewandowski AJ, Holloway CJ, et al. Observational study of regional aortic size referenced to body size: production of a cardiovascular magnetic resonance nomogram. *J Cardiovasc Magn Reson* 2014;16:9. DOI PubMed PMC
24. Murillo H, Lane MJ, Punn R, Fleischmann D, Restrepo CS. Imaging of the aorta: embryology and anatomy. *Semin Ultrasound CT*

*MR* 2012;33:169-90. DOI PubMed

25. Grewal N, Gittenberger-de Groot AC, Lindeman JH, et al. Normal and abnormal development of the aortic valve and ascending aortic wall: a comprehensive overview of the embryology and pathology of the bicuspid aortic valve. *Ann Cardiothorac Surg* 2022;11:380-8. DOI PubMed PMC
26. Koc AS, Sumbul HE. Increased aortic intima-media thickness may be used to detect macrovascular complications in adult type II diabetes mellitus patients. *Cardiovasc Ultrasound* 2018;16:8. DOI PubMed PMC
27. Järvisalo MJ, Jartti L, Näntö-Salonen K, et al. Increased aortic intima-media thickness: a marker of preclinical atherosclerosis in high-risk children. *Circulation* 2001;104:2943-7. DOI
28. Davis PH, Dawson JD, Blecha MB, Mastbergen RK, Sonka M. Measurement of aortic intimal-medial thickness in adolescents and young adults. *Ultrasound Med Biol* 2010;36:560-5. DOI PubMed PMC
29. Ender J, Singh R, Nakahira J, Subramanian S, Thiele H, Mukherjee C. Echo didactic: visualization of the circumflex artery in the perioperative setting with transesophageal echocardiography. *Anesth Analg* 2012;115:22-6. DOI PubMed
30. Maxwell C, Cherry A, Daneshmand M, Swaminathan M, Nicoara A. Assessment of coronary blood flow by transesophageal echocardiography. *J Cardiothorac Vasc Anesth* 2016;30:258-60. DOI PubMed
31. Salerno P, Jackson A, Shaw M, Spratt P, Jansz P. Transesophageal echocardiographic imaging of the branches of the aorta: a guide to obtaining these images and their clinical utility. *J Cardiothorac Vasc Anesth* 2009;23:694-701. DOI PubMed
32. Kondo N, Hirose N, Kihara K, Tashiro M, Miyashita K, Orihashi K. Intraoperative transesophageal echocardiography for coronary artery assessment. *Circ Rep* 2020;2:517-25. DOI PubMed PMC
33. Hagendorff A, Evangelista A, Fehske W, Schäfers HJ. Improvement in the assessment of aortic valve and aortic aneurysm repair by 3-dimensional echocardiography. *JACC Cardiovasc Imaging* 2019;12:2225-44. DOI PubMed
34. Faletra FF, Agricola E, Flachskampf FA, et al. Three-dimensional transoesophageal echocardiography: how to use and when to use-a clinical consensus statement from the European Association of Cardiovascular Imaging of the European Society of Cardiology. *Eur Heart J Cardiovasc Imaging* 2023;24:e119-97. DOI
35. van Zaane B, Nierich AP, Buhre WF, Brandon Bravo Bruinsma GJ, Moons KG. Resolving the blind spot of transoesophageal echocardiography: a new diagnostic device for visualizing the ascending aorta in cardiac surgery. *Br J Anaesth* 2007;98:434-41. DOI PubMed
36. Nierich AP, van Zaane B, Buhre WF, Coddens J, Spanjersberg AJ, Moons KG. Visualization of the distal ascending aorta with A-mode transesophageal echocardiography. *J Cardiothorac Vasc Anesth* 2008;22:766-73. DOI PubMed
37. Glas KE, Swaminathan M, Reeves ST, et al; Council for Intraoperative Echocardiography of the American Society of Echocardiography; Society of Cardiovascular Anesthesiologists. Guidelines for the performance of a comprehensive intraoperative epiaortic ultrasonographic examination: recommendations of the American Society of Echocardiography and the Society of Cardiovascular Anesthesiologists; endorsed by the Society of Thoracic Surgeons. *J Am Soc Echocardiogr* 2007;20:1227-35. DOI
38. Orihashi K, Matsuura Y, Sueda T, et al. Aortic arch branches are no longer a blind zone for transesophageal echocardiography: a new eye for aortic surgeons. *J Thorac Cardiovasc Surg* 2000;120:466-72. DOI
39. Agrawal G, LaMotte LC, Nanda NC, Parekh HH. Identification of the aortic arch branches using transesophageal echocardiography. *Echocardiography* 1997;14:461-6. DOI PubMed
40. Patil TA, Ambli SK. Transesophageal echocardiography evaluation of the aortic arch branches. *Ann Card Anaesth* 2018;21:53-6. DOI PubMed PMC
41. Ravi BS, Nanda NC, Htay T, Dod HS, Agrawal G. Transesophageal echocardiographic identification of normal and stenosed posterior intercostal arteries. *Echocardiography* 2003;20:609-15. DOI PubMed
42. Howard A, Jackson A, Howard C, Spratt P. Estimating the volume of chronic pleural effusions using transesophageal echocardiography. *J Cardiothorac Vasc Anesth* 2011;25:229-32. DOI PubMed
43. Capper SJ, Ross JJ, Sandström E, Braidley PC, Morgan-Hughes NJ. Transoesophageal echocardiography for the detection and quantification of pleural fluid in cardiac surgical patients. *Br J Anaesth* 2007;98:442-6. DOI PubMed
44. Rodríguez-Palomares JF, Teixidó-Tura G, Galuppo V, et al. Multimodality assessment of ascending aortic diameters: comparison of different measurement methods. *J Am Soc Echocardiogr* 2016;29:819-26.e4. DOI
45. Lang RM, Badano LP, Mor-Avi V, et al. Recommendations for cardiac chamber quantification by echocardiography in adults: an update from the American Society of Echocardiography and the European Association of Cardiovascular Imaging. *J Am Soc Echocardiogr* 2015;28:1-39.e14. DOI
46. Muraru D, Maffessanti F, Kocabay G, et al. Ascending aorta diameters measured by echocardiography using both leading edge-to-leading edge and inner edge-to-inner edge conventions in healthy volunteers. *Eur Heart J Cardiovasc Imaging* 2014;15:415-22. DOI
47. Otto CM, Nishimura RA, Bonow RO, et al. 2020 ACC/AHA guideline for the management of patients with valvular heart disease: executive summary: a report of the American College of Cardiology/American Heart Association Joint Committee on clinical practice guidelines. *Circulation* 2021;143:e35-71. DOI
48. Van Dyck MJ, Watremez C, Boodhwani M, Vanoverschelde JL, El Khoury G. Transesophageal echocardiographic evaluation during aortic valve repair surgery. *Anesth Analg* 2010;111:59-70. DOI PubMed
49. Ouzounian M, Hage A, Chung J, et al; Canadian Thoracic Aortic Collaborative. Hybrid arch frozen elephant trunk repair: evidence from the Canadian Thoracic Aortic Collaborative. *Ann Cardiothorac Surg* 2020;9:189-96. DOI PubMed PMC
50. Wallet F, Perbet S, Fléron MH, et al. Elephant trunk prosthesis kinking: transesophageal echocardiography diagnosis. *Anesth Analg*

2008;106:67-9. DOI

51. Kayali F, Qutaishat S, Jubouri M, Chikhal R, Tan SZCP, Bashir M. Kinking of frozen elephant trunk hybrid prostheses: incidence, mechanism, and management. *Front Cardiovasc Med* 2022;9:912071. DOI PubMed PMC
52. Kronzon I, Tunick PA. Aortic atherosclerotic disease and stroke. *Circulation* 2006;114:63-75. DOI PubMed
53. Knol WG, Budde RPJ, Mahtab EAF, Bekkers JA, Bogers AJJC. Intimal aortic atherosclerosis in cardiac surgery: surgical strategies to prevent embolic stroke. *Eur J Cardiothorac Surg* 2021;60:1259-67. DOI PubMed PMC
54. Cohen A, Donal E, Delgado V, et al; Reviewers: this document was reviewed by members of the 2018-2020 EACVI Scientific Documents Committee; chair of the 2018-2020 EACVI Scientific Documents Committee. EACVI recommendations on cardiovascular imaging for the detection of embolic sources: endorsed by the Canadian Society of Echocardiography. *Eur Heart J Cardiovasc Imaging* 2021;22:e24-57. DOI
55. Evangelista A, Flachskampf FA, Erbel R, et al. Echocardiography in aortic diseases: EAE recommendations for clinical practice. *Eur J Echocardiogr* 2010;11:645-58. DOI
56. Klomp WW, Brandon Bravo Bruinsma GJ, van't Hof AW, Grandjean JG, Nierich AP. Imaging techniques for diagnosis of thoracic aortic atherosclerosis. *Int J Vasc Med* 2016;2016:4726094. DOI PubMed PMC
57. Ito A, Sugioka K, Matsumura Y, et al. Rapid and accurate assessment of aortic arch atherosclerosis using simultaneous multi-plane imaging by transesophageal echocardiography. *Ultrasound Med Biol* 2013;39:1337-42. DOI
58. Shimokawa T, Minato N, Yamada N, Takeda Y, Hisamatsu Y, Itoh M. Assessment of ascending aorta using epiaortic ultrasonography during off-pump coronary artery bypass grafting. *Ann Thorac Surg* 2002;74:2097-100. DOI PubMed
59. Biancari F, Santini F, Tauriainen T, et al. Epiaortic ultrasound to prevent stroke in coronary artery bypass grafting. *Ann Thorac Surg* 2020;109:294-301. DOI
60. Shapeton AD, Leissner KB, Zorca SM, et al. Epiaortic ultrasound for assessment of intraluminal atheroma; insights from the REGROUP trial. *J Cardiothorac Vasc Anesth* 2020;34:726-32. DOI PubMed PMC
61. Paruchuri V, Salhab KF, Kuzmik G, et al. Aortic size distribution in the general population: explaining the size paradox in aortic dissection. *Cardiology* 2015;131:265-72. DOI
62. Isselbacher EM, Preventza O, Hamilton Black J 3rd, et al. 2022 ACC/AHA guideline for the diagnosis and management of aortic disease: a report of the American Heart Association/American College of Cardiology Joint Committee on clinical practice guidelines. *Circulation* 2022;146:e334-482. DOI
63. Pinard A, Jones GT, Milewicz DM. Genetics of thoracic and abdominal aortic diseases. *Circ Res* 2019;124:588-606. DOI PubMed PMC
64. Boodhwani M, de Kerchove L, Glineur D, et al. Repair-oriented classification of aortic insufficiency: impact on surgical techniques and clinical outcomes. *J Thorac Cardiovasc Surg* 2009;137:286-94. DOI
65. Weinreich M, Yu PJ, Trost B. Sinus of valsalva aneurysms: review of the literature and an update on management. *Clin Cardiol* 2015;38:185-9. DOI PubMed PMC
66. Carrel T, Sundt TM 3rd, von Kodolitsch Y, Czerny M. Acute aortic dissection. *Lancet* 2023;401:773-88. DOI PubMed
67. Rylski B, Schilling O, Czerny M. Acute aortic dissection: evidence, uncertainties, and future therapies. *Eur Heart J* 2023;44:813-21. DOI PubMed
68. Meredith EL, Masani ND. Echocardiography in the emergency assessment of acute aortic syndromes. *Eur J Echocardiogr* 2009;10:i31-9. DOI PubMed
69. Evangelista A, Aguilar R, Cuellar H, et al. Usefulness of real-time three-dimensional transoesophageal echocardiography in the assessment of chronic aortic dissection. *Eur J Echocardiogr* 2011;12:272-7. DOI
70. Wang CJ, Rodriguez Diaz CA, Trinh MA. Use of real-time three-dimensional transesophageal echocardiography in type A aortic dissections: advantages of 3D TEE illustrated in three cases. *Ann Card Anaesth* 2015;18:83-6. DOI PubMed PMC
71. Kitamura T, Nie M, Horai T, Miyaji K. Direct true lumen cannulation ("Samurai" cannulation) for acute stanford type A aortic dissection. *Ann Thorac Surg* 2017;104:e459-61. DOI PubMed
72. Flachskampf FA, Badano L, Daniel WG, et al. Recommendations for transoesophageal echocardiography: update 2010. *Eur J Echocardiogr* 2010;11:557-76. DOI
73. Patel PA, Bavaria JE, Ghadimi K, et al. Aortic regurgitation in acute type-A aortic dissection: a clinical classification for the perioperative echocardiographer in the era of the functional aortic annulus. *J Cardiothorac Vasc Anesth* 2018;32:586-97. DOI
74. Makhija N, Magoon R, Sarkar S. Transesophageal echocardiographic imaging of an aortic intramural hematoma: characterizing the crescent. *Can J Anaesth* 2019;66:1415-6. DOI PubMed
75. Machelart I, Greib C, Wirth G, et al. Graft infection after a Bentall procedure: a case series and systematic review of the literature. *Diagn Microbiol Infect Dis* 2017;88:158-62. DOI
76. Ram H, Dwarakanath S, Green AE, Steyn J, Hessel EA 2nd. Iatrogenic aortic dissection associated with cardiac surgery: a narrative review. *J Cardiothorac Vasc Anesth* 2021;35:3050-66. DOI PubMed
77. Ram H, Weaver AR, Dorfling J. Iatrogenic aortic intramural hematoma: guidance to intraoperative decision making: a case report. *A A Pract* 2020;14:e01191. DOI PubMed
78. Muhyieddeen K, Samim A, Roberts M, Srikanth S. A case of iatrogenic aortic intramural hematoma. *Methodist Debakey Cardiovasc J* 2017;13:37-8. DOI PubMed PMC
79. Welch TD, Foley T, Barsness GW, et al. Iatrogenic aortic dissection ... or intramural hematoma? *Circulation* 2012;125:e415-8. DOI

80. Vignon P, Guéret P, Vedrinne JM, et al. Role of transesophageal echocardiography in the diagnosis and management of traumatic aortic disruption. *Circulation* 1995;92:2959-68. DOI
81. Miller-Hance WC, Silverman NH. Transesophageal echocardiography (TEE) in congenital heart disease with focus on the adult. *Cardiol Clin* 2000;18:861-92. DOI PubMed
82. Cardoso G, Abecasis M, Anjos R, et al. Aortic coarctation repair in the adult. *J Card Surg* 2014;29:512-8. DOI
83. Duffy CI, Plehn JF. Transesophageal echocardiographic assessment of aortic coarctation using color, flow-directed Doppler sampling. *Chest* 1994;105:286-8. DOI PubMed
84. Singh S, Hakim FA, Sharma A, et al. Hypoplasia, pseudocoarctation and coarctation of the aorta - a systematic review. *Heart Lung Circ* 2015;24:110-8. DOI
85. Habib G, Badano L, Tribouilloy C, et al; European Association of Echocardiography. Recommendations for the practice of echocardiography in infective endocarditis. *Eur J Echocardiogr* 2010;11:202-19. DOI
86. Bruun NE, Habib G, Thuny F, Sogaard P. Cardiac imaging in infectious endocarditis. *Eur Heart J* 2014;35:624-32. DOI PubMed
87. Mohananey D, Mohadjer A, Pettersson G, et al. Association of vegetation size with embolic risk in patients with infective endocarditis: a systematic review and meta-analysis. *JAMA Intern Med* 2018;178:502-10. DOI PubMed PMC
88. Deprèle C, Berthelot P, Lemetayer F, et al. Risk factors for systemic emboli in infective endocarditis. *Clin Microbiol Infect* 2004;10:46-53. DOI
89. Di Salvo G, Habib G, Pergola V. Echocardiography predicts embolic events in infective endocarditis. *J Am Coll Cardiol* 2001;37:1069-76. DOI
90. Habib G, Lancellotti P, Antunes MJ, et al; ESC Scientific Document Group. 2015 ESC guidelines for the management of infective endocarditis: the task force for the management of infective endocarditis of the European Society of Cardiology (ESC). Endorsed by: European Association for Cardio-Thoracic Surgery (EACTS), the European Association of Nuclear Medicine (EANM). *Eur Heart J* 2015;36:3075-128. DOI
91. Berdejo J, Shibayama K, Harada K, et al. Evaluation of vegetation size and its relationship with embolism in infective endocarditis: a real-time 3-dimensional transesophageal echocardiography study. *Circ Cardiovasc Imaging* 2014;7:149-54. DOI
92. Hermanns H, Eberl S, Terwindt LE, et al. Anesthesia considerations in infective endocarditis. *Anesthesiology* 2022;136:633-56. DOI
93. Anguera I, Miro JM, Vilacosta I; Aorto-cavitary Fistula in Endocarditis Working Group. Aorto-cavitary fistulous tract formation in infective endocarditis: clinical and echocardiographic features of 76 cases and risk factors for mortality. *Eur Heart J* 2005;26:288-97. DOI
94. Shapira Y, Weisenberg DE, Vaturi M, et al. The impact of intraoperative transesophageal echocardiography in infective endocarditis. *Isr Med Assoc J* 2007;9:299-302. Available from: https://www.ima.org.il/MedicineIMAJ/viewarticle.aspx?year=2007&month=04&page=299 [Last accessed on 22 Dec 2023].
95. Wilson WR, Bower TC, Creager MA, et al. Vascular graft infections, mycotic aneurysms, and endovascular infections: a scientific statement from the American Heart Association. *Circulation* 2016;134:e412-60. DOI
96. Van Hemelrijck MV, Sromicki J, Husmann L, Rancic Z, Hasse B, Carrel TP. Vascular graft infections. *Vessel Plus* 2022;6:47. DOI
97. Uslu A, Kup A, Güner A, et al. Multimodality imaging of an aortic graft infection. *Echocardiography* 2019;36:2271-3. DOI
98. Upchurch GR, Escobar GA, Azizzadeh A, et al. Society for vascular surgery clinical practice guidelines of thoracic endovascular aortic repair for descending thoracic aortic aneurysms. *J Vasc Surg* 2021;73:55S-83S. DOI
99. Czerny M, Pacini D, Aboyans V, et al. Current options and recommendations for the use of thoracic endovascular aortic repair in acute and chronic thoracic aortic disease: an expert consensus document of the European Society for Cardiology (ESC) Working Group of Cardiovascular Surgery, the ESC Working Group on Aorta and Peripheral Vascular Diseases, the European Association of Percutaneous Cardiovascular Interventions (EAPCI) of the ESC and the European Association for Cardio-Thoracic Surgery (EACTS). *Eur J Cardiothorac Surg* 2021;59:65-73. DOI
100. Czerny M, Schmidli J, Adler S, et al; EACTS/ESVS scientific document group. Current options and recommendations for the treatment of thoracic aortic pathologies involving the aortic arch: an expert consensus document of the European Association for Cardio-Thoracic surgery (EACTS) and the European Society for Vascular Surgery (ESVS). *Eur J Cardiothorac Surg* 2019;55:133-62. DOI
101. Rocchi G, Lofiego C, Biagini E, et al. Transesophageal echocardiography-guided algorithm for stent-graft implantation in aortic dissection. *J Vasc Surg* 2004;40:880-5. DOI
102. Rapezzi C, Rocchi G, Fattori R, et al. Usefulness of transesophageal echocardiographic monitoring to improve the outcome of stent-graft treatment of thoracic aortic aneurysms. *Am J Cardiol* 2001;87:315-9. DOI
103. Fattori R, Caldarera I, Rapezzi C, et al. Primary endoleakage in endovascular treatment of the thoracic aorta: importance of intraoperative transesophageal echocardiography. *J Thorac Cardiovasc Surg* 2000;120:490-5. DOI
104. Reformato V, Taylor B, Kaczorowski D, Mazzeffi M. Transesophageal echocardiography for ascending thoracic endovascular aortic repair of stanford type A aortic dissection. *A A Pract* 2019;13:78-80. DOI PubMed
105. Preventza O, Le Huu A, Olive J, Cekmecelioglu D, Coselli JS. Endovascular repair of the ascending aorta: the last frontier. *Ann Cardiothorac Surg* 2022;11:26-30. DOI PubMed PMC
106. Garrido JM, Ferreiro-Marzal A, Esteban-Molina M, Rodríguez-Morata A, Rodríguez-Serrano F. Endovascular technique for ascending aorta repair based on TEVAR and TAVI procedures. *J Endovasc Ther* 2023:15266028221148383. DOI PubMed
107. Roselli EE, Idrees JJ, Johnston DR, Eagleton MJ, Desai MY, Svensson LG. Zone zero thoracic endovascular aortic repair: a proposed

modification to the classification of landing zones. *J Thorac Cardiovasc Surg* 2018;155:1381-9. DOI

108. Wipper SH, Kölbel T, Dumfarth J, et al. A new hybrid graft for open thoracoabdominal aortic aneurysm repair. *Ann Cardiothorac Surg* 2023;12:503-5. DOI PubMed PMC
109. Debus ES, Malik K, Kölbel T, et al. First in human implantation of the thoracoflo graft: a new hybrid device for thoraco-abdominal aortic repair. *EJVES Vasc Forum* 2023;58:28-31. DOI PubMed PMC
110. Nyrnes SA, Fadnes S, Wigen MS, Mertens L, Lovstakken L. Blood speckle-tracking based on high-frame rate ultrasound imaging in pediatric cardiology. *J Am Soc Echocardiogr* 2020;33:493-503.e5. DOI PubMed
111. Fadnes S, Wigen MS, Nyrnes SA, Lovstakken L. In vivo intracardiac vector flow imaging using phased array transducers for pediatric cardiology. *IEEE Trans Ultrason Ferroelectr Freq Control* 2017;64:1318-26. DOI PubMed
112. Sørensen K, Fadnes S, Mertens L, et al. Assessment of early diastolic intraventricular pressure difference in children by blood speckle-tracking echocardiography. *J Am Soc Echocardiogr* 2023;36:523-32.e3. DOI
113. Wigen MS, Fadnes S, Rodriguez-Molares A, et al. 4-D intracardiac ultrasound vector flow imaging-feasibility and comparison to phase-contrast MRI. *IEEE Trans Med Imaging* 2018;37:2619-29. DOI
114. Lowe C, Abbas A, Rogers S, Smith L, Ghosh J, McCollum C. Three-dimensional contrast-enhanced ultrasound improves endoleak detection and classification after endovascular aneurysm repair. *J Vasc Surg* 2017;65:1453-9. DOI PubMed
115. Agricola E, Slavich M, Rinaldi E, et al. Usefulness of contrast-enhanced transoesophageal echocardiography to guide thoracic endovascular aortic repair procedure. *Eur Heart J Cardiovasc Imaging* 2016;17:67-75. DOI
116. Agricola E, Slavich M, Bertoglio L, et al. Contrast-enhanced TEE during thoracic endovascular aortic repair procedure. *JACC Cardiovasc Imaging* 2015;8:980-2. DOI
117. Rylski B, Szeto WY, Bavaria JE, Branchetti E, Moser W, Milewski RK. Development of a single endovascular device for aortic valve replacement and ascending aortic repair. *J Card Surg* 2014;29:371-6. DOI PubMed
118. Felipe Gaia D, Bernal O, Castilho E, et al. First-in-human endo-bentall procedure for simultaneous treatment of the ascending aorta and aortic valve. *JACC Case Rep* 2020;2:480-5. DOI PubMed PMC
119. Gandet T, Westermann D, Conradi L, et al. Modular endo-bentall procedure using a “rendez-vous access”. *J Endovasc Ther* 2022;29:711-6. DOI
120. Leshnower BG, Duwayri YM, Nicholson WJ, et al. Endo-bentall procedure using off-the-shelf catheter devices to repair an aorto-atrial fistula. *Circ Cardiovasc Interv* 2023;16:e012848. DOI